American Journal of Pathology, Vol. 164, No. 5, May 2004

N-Acetyl-Cysteine Promotes Angiostatin Production and Vascular Collapse in an Orthotopic Model of Breast Cancer

Anshu Agarwal,* Ursula Muñoz-Nájar,* Ulrike Klueh,† Shu-Ching Shih,‡ and Kevin P. Claffey*

From the Departments of Physiology and Pathology,† University of Connecticut Health Center, Farmington, Connecticut; and the Department of Ophthalmology,‡ Children's Hospital and Harvard Medical School, Boston, Massachusetts*

The antioxidant *N*-acetyl-cysteine (NAC) has been shown to be chemopreventive in clinical studies, and in recent studies, has shown promise in preventing tumor progression. Although the effects of NAC on tumorigenesis have been associated with decreased angiogenesis, the mechanism of the anti-angiogenic activity has not been determined. In the following study, we describe a novel mechanism whereby NAC therapy blocks MDA-MB-435 breast carcinoma cell proliferation and metastasis in an *in vivo* tumorigenic model. Athymic nude mice bearing MDA-MB-435 xenografts were treated with systemic NAC daily for 8 weeks. NAC treatment resulted in endothelial cell apoptosis and reduction of microvascular density within the core of the tumor leading to significant tumor cell apoptosis/necrosis. Angiostatin accumulated in tumors from NAC-treated but not control animals. Additional studies using a vascular endothelial growth factor-dependent chicken chorioallantoic membrane angiogenic assay recapitulated NAC-induced endothelial apoptosis and coordinate production of angiostatin, a potent endothelial apoptotic factor. *In vitro* studies showed angiostatin was formed in endothelial cultures in a vascular endothelial growth factor- and NAC-dependent manner, a process that requires endothelial cell surface plasminogen activation. These results suggest that systemic NAC therapy promotes anti-angiogenesis through angiostatin production, resulting in endothelial apoptosis and vascular collapse in the tumor. *(Am J Pathol 2004, 164:1683–1696)*

Solid tumor progression and metastasis has been tightly linked to tumor-induced neovascularization or angiogenesis.[1,2] Vascular endothelial growth factor (VEGF) is one of the most potent angiogenic factors elicited by most solid tumors in breast and other cancers.[3–5] The expression of VEGF has been demonstrated to be a significant factor correlating with poor prognosis and metastatic relapse in breast, ovarian, and pancreatic cancers.[6–9] Control of VEGF expression is unique in that it is mediated through multiple pathways within tumor microenvironments such as nutrient depletion (hypoglycemia and hypoxia), cytokine activation [transforming growth factor-β, tumor necrosis factor-α, and fibroblast growth factor (FGF-2)], signal transduction pathway activation (ras, nuclear factor-κB, and PKC), as well as by cell-damaging agents (UV, reactive oxygen species, and carcinogens).[10–15] VEGF activation of endothelial cells results in acute vascular permeability, promotion of inflammatory cell infiltration through adhesion molecule expression (ie, E-selectin and ICAM-1), and induction of a proliferative and migratory phenotype.[16–19] In addition, VEGF can induce endothelial cell urokinase plasminogen activator/urokinase plasminogen activator receptor (uPA/uPAR) expression resulting in the focal activation of plasminogen into plasmin.[20–23] Plasmin promotes basement membrane modification and induction of adhesion substrates for integrin-dependent endothelial cell migration,[24–26] a process essential to angiogenesis. Given the potency of VEGF to drive endothelial cell migration and promote angiogenesis, VEGF has been selectively targeted for anti-tumorigenic efficacy.

Anti-angiogenic factors that counterbalance the proangiogenic events in tumors include matrix components such as thrombospondins[27] and laminin, as well as proteolytic byproducts such as angiostatin, endostatin, and tumstatin.[28–31] Interestingly, angiostatin was discovered to be a unique fragment of plasminogen with potent apoptotic activity toward endothelial cells. The mechanism of action of angiostatin may include inhibition of endothelial cell surface F(1)-F(0) ATP synthase,[32,33] blocking growth promoting ERK-1 and ERK-2 signal transduction cascades, and/or modification of cellular pH balance.[34,35]

N-acetyl-cysteine (NAC) is an analogue and precursor of glutathione, an intracellular protective reducing equivalent.

Supported by the National Cancer Institute (CA064436) and the National Heart, Lung, and Blood Institute (PO1-HL70694-01).

Accepted for publication January 26, 2004.

Address reprint requests to Kevin Claffey, Ph.D., Department of Physiology, Center for Vascular Biology, University of Connecticut Health Center, 263 Farmington Ave., Farmington, CT 06030-3501. E-mail: claffey@nso2.uchc.edu.

The antioxidant activity of NAC may have an important role as a chemopreventive agent for cancer progression because of its protective effect against UV-induced cellular damage.[36,37] Several investigations have indicated that NAC prevents the induction and maintenance of DNA damage and progression to cancer in smokers.[38] At the cellular level, NAC has been shown to inhibit endothelial cell invasion and angiogenesis *in vitro*, presumably because of the inhibition of metalloproteinase activities.[39] Conversely, NAC has been shown to have cytoprotective and anti-genotoxic effects on endothelial cells directly.[40] The chemopreventive activities of NAC have been shown to block tumor growth and angiogenesis in athymic nude mice.[41] Interestingly, NAC therapy was found to be synergistic with doxorubicin in blocking experimental tumorigenesis.[41,42] NAC has also been shown to modulate transcriptional activities through several pathways involving c-fos/c-jun, nuclear factor-κB, STAT, and cyclin inhibitors.[43] Given the possible connection between NAC treatment and reductions in tumor-dependent angiogenesis, it has been reported that one important aspect of NAC effectiveness is to limit the expression of VEGF.[44] This effect seems to be related to possible repression of reactive oxygen species and limiting hypoxia-induced transcription through hypoxia inducible factor-1.[15] Interestingly, it has been shown that the conversion of plasminogen into plasmin by cellular-derived plasminogen activators (uPA, tPA) in the presence of NAC, results in the accumulation of angiostatin *in vitro*.[45] The possibility that angiostatin formation can be promoted by NAC in which plasminogen activation occurs might provide additional mechanisms whereby antioxidant therapies could affect tumor angiogenesis *in vivo*.

The idea that the tumor microenvironment and the dependence on vascular maintenance within tumors can be modulated by nontoxic, well-tolerated antioxidants is exciting and may have enormous potential in reducing breast cancer progression and metastasis. Here, it was determined that effectiveness of NAC therapy on breast cancer progression was selective to a specific tumor size in which tumors are angiogenesis-dependent. The VEGF-dependent endothelial apoptosis in the presence of NAC was directly related to the production of the endothelial apoptotic factor, angiostatin. This study has defined a novel mechanism by which NAC has anti-angiogenic activity that is dependent on VEGF activation of endothelial cells, resulting in angiostatin-induced endothelial apoptosis, vessel regression, and intratumoral necrosis. Thus, nontoxic antioxidants such as NAC, can modulate tumor angiogenesis by promoting the formation of the endogenous anti-angiogenic molecule, angiostatin.

Materials and Methods

Cell Lines and Culture Conditions

The MDA-MB-435[46] cell line (American Type Culture Collection, Manassas, VA) was cultured in Dulbecco's Modified Eagle's Medium (DMEM) supplemented with 10% fetal bovine serum (FBS, Invitrogen, San Diego, CA). Parental cells were transfected with pcDNA3.1/Neo (Invitrogen) vector expressing enhanced green fluorescent protein (EGFP) and selected with 850 μg/ml of Geneticin or G418.[47] Stable clones were maintained in 250 μg/ml of G418 and evaluated for invasive capacity using modified Boyden chambers coated with Matrigel (BD Biosciences, Heidelberg, Germany) as described previously.[48] MDA-MB-435 tumor cell experimental conditions of normoxia (21% O_2) and hypoxia (3% O_2) were performed in humidified incubators with 5% CO_2 in the presence of 1% FBS for chronic stress events. Primary low-passage human umbilical vein endothelial cells (HUVECs, a gift of Dr. Tim Hla, University of Connecticut Health Center, Department of Physiology) were cultured as described previously.[49,50] Growth media was restricted to MEM 199 (Invitrogen) with 0.5 to 3% FBS for experimental conditions.

Human Orthotopic Xenograft Breast Cancer Model with MDA-MB-435 Cells Expressing Green Fluorescent Protein (GFP)

Tumorigenic profiles of 12 different stable MDA-MB-435-GFP clones were evaluated for growth of 1×10^6 cells injected subcutaneously in the mammary fat pad of female athymic (nu/nu) mice and tumor growth determined throughout 8 weeks by external caliper measurements of tumor and calculated as width^2 $\times$ length $\times$ 0.52 to approximate ellipsoid structure. A single clone demonstrating uniform tumor inoculation (100%), low-growth rate variability, and reproducible lymph node and lung metastases was chosen for further use, as described previously.[47] Animals bearing tumors were treated by subcutaneous injection of sterile saline or NAC (Sigma, St. Louis, MO) in saline at the indicated dose. Injections were performed daily without evidence of animal weight loss, injection site irritation, or other adverse signs of poor health. Animal studies were performed at least three times with an average treatment group size of 10 animals per experiment. Tumor metastasis to lymph node and lung were evaluated by fluorescence microscopy in which intrinsic background was reduced by intracardiac perfusion of animals with phosphate-buffered saline (PBS) followed by 3.7% paraformaldehyde in PBS to fix all tissues. Tumor, axial lymph nodes, lungs, spleen, liver, and bone were removed and washed in PBS. Gross organ evaluation for GFP-expressing foci were performed with a Zeiss Axioplan 2 fluorescent microscope or a laser-scanning confocal microscope (Zeiss LZM-410, Thornwood, NY). Tissues were then incubated in 0.3 mol/L sucrose:PBS overnight at 4°C and embedded into OCT cryosectioning media and frozen at −80°C. Frozen blocks were cryosectioned (10 to 15 μm), postfixed with methanol:acetone (1:1, −20°C) for 10 minutes, and rehydrated with PBS/1 mmol/L $MgCl_2$ for 15 minutes. The sections were coverslipped in PBS:glycerol (1:1) and analyzed for fluorescence using either direct fluorescent microscopy or confocal as needed.

Immunohistochemistry

Cryosections and postfixed slides were used for immunohistochemical analyses with antibodies to platelet

endothelial cell adhesion molecule PECAM-1 (Pharmingen, San Diego, CA), angiostatin (purified rabbit anti-human angiostatin peptide, Ab2904; Novus Biologicals, Littleton, CO), human VEGF-165 (R&D Systems, Inc., Minneapolis, MN), and apoptosis with ApopTag TUNEL kit (Intergen, Purchase, NY). Secondary detection was performed with appropriate biotinylated secondary antibodies and VectaStain Elite kit (Vector, Inc., Burlingame, CA) with diaminobenzidine substrate. Counterstain was performed with 1% methyl green. Negative control slides were obtained by omitting the primary antibody. The images were quantified by counting vessels/cells using image analysis and recognition software, Image Pro Plus (Media Cybernetics, L.P., Silver Spring, MD), and averaged for three high-power fields/section/animal for 10 animals/group for each treatment group.

Endothelial Cell Proliferation and Viability Assays

Cells were seeded in triplicate for each treatment at a cell density of 1×10^4 cells/ml into plates containing complete media (10% FBS) and allowed to grow to 80 to 90% confluency. Treatment conditions were as indicated in 0.5 to 3% FBS with NAC and recombinant hVEGF-165 or FGF-2 (R&D Systems), *S*-adenosyl-methionine (SAM) (Sigma), sphingosine-1-phosphate (Biomol, Plymouth Meeting, PA), PAI-1 and TIMP-2 (Calbiochem, San Diego, CA), or antibody to angiostatin (rabbit anti-human angiostatin; Alpha Diagnostics, (San Antonio, TX) or Oncogene Research Products, San Diego, CA). Cells were harvested from 1 to 3 days later and quantified by complete trypsinization and Coulter counting (Beckman Coulter, Miami, FL). Cell viability was assessed by addition of MTT (100 μg/ml, Sigma) to the cell culture, incubation for 2 hours, solubilization (10% Triton X-100, 0.1 N HCl in isopropanol) and quantification by spectrophotometric absorbance measurement at 570 nm. Results are expressed as mean $\pm$ SD.

Protein Expression

Protein extracts from dissected MDA-MB-435 tumors or membranes dissected from CAMs combined from three sites, were obtained using fivefold volumes of 1% Triton X-100 lysis buffer (1% Triton X-100, 50 mmol/L Hepes, pH 7.5, 150 mmol/L NaCl, 1 mmol/L EGTA, 10 mmol/L sodium pyrophosphate, 100 mmol/L NaF, 0.2 mmol/L $NaOVa_4$, 10% glycerol, and 5 mmol/L 4-(2-aminoethyl-)benzene-sulfonyl fluoride) and homogenizing with a motorized tissue grinder (Polytron; Brinkman, Westbury, NY). Homogenates were centrifuged at 3000 $\times$ *g* to remove debris and nuclei. Samples were stored until assayed at -80°C and protein concentration determined using Bio-Rad DC protein assay (Bio-Rad, Richmond, CA) using bovine serum albumin as control. VEGF enzyme-linked immunosorbent assays were performed on total tumor extracts as described previously.[13] Anti-human VEGF polyclonal chicken antibodies were bound to plates overnight at 2.5 μg/ml, washed in PBS/0.05% Tween-20 and plates blocked with 2% normal human serum. Samples were serially diluted in PBS/0.05% Tween-20 and bound for 2 hours at 37°C, washed, and anti-mouse or anti-human VEGF antibody (1.5 μg/ml; R&D Systems, Inc.)-bound for 2 hours at room temperature. Detection was achieved by binding secondary horseradish peroxidase conjugate at 1 μg/ml for 30 minutes, addition of soluble horseradish peroxidase TMB substrate (KPL, Inc., Gaithersburg, MD), acidification with equal volume 0.18 N H_2SO_4, and optical density reading at 450 nm. Human recombinant VEGF (R&D Systems, Inc.) was used as a positive quantitative control. Conditioned medias from HUVEC experiments were concentrated by 5 vol using Amicon Centricon-10 microconcentrators. ImmunoBlots were performed using anti-angiostatin (Calbiochem, or Oncogene Research Products) or anti-β-actin (Sigma) antibodies under nondenaturing conditions with 40 μg of protein in 10% sodium dodecyl sulfate-polyacrylamide gel electrophoresis gels. Detection was performed using secondary horseradish peroxidase-conjugated antibodies and enhanced chemiluminescence substrate (KPL, Inc.). β-Actin levels did not show regulation by NAC treatment and served as a control for the immunoblot analysis.

RNA Analysis

For RNA isolation, tumor tissue was dissected and immediately lysed in RNA lysis buffer from RNAeasy kit (Qiagen, Valencia, CA) and processed according to the manufacturer's instructions. RNAs were quantified by absorbance 260/280 nm and a qualitative Northern blot was performed to assure RNA of high quality (28s $>$ 18s ribosomal RNAs under ethidium bromide illumination). Northern blots were analyzed for human VEGF, glucose transporter-1 (Glut-1), and control ribosome-associated protein (36B4) as defined previously.[13,51] The signals for VEGF and Glut-1 were normalized to 36B4 in each lane using PhosphorImager and ImageQuant software (Molecular Dynamics, Sunnyvale, CA).

cDNA Preparation and Real-Time Reverse Transcriptase-Polymerase Chain Reaction (RT-PCR) Analysis of Gene Expression

Total RNA (100 ng) from tumor samples were converted into cDNA using murine leukemia virus reverse transcriptase (Life Technologies, Inc., Bethesda, MD) as described previously.[52] Real-time PCR primers targeting murine PECAM-1, murine VEGF, murine cyclophilin, human VEGF, and human cyclophilin were designed using Primer Express software (Applied BioSystems, Foster City, CA) and synthesized by Genemed Synthesis, South San Francisco, CA. Murine and human VEGF primers detected all alternative splice forms of the mRNA. Cyclophilin expression was unchanged in all tumor samples tested and was used to normalize gene-specific signal. Specificity of each primer was confirmed by NCBI Blast analysis and efficacy assured by testing amplicons from PCR reactions for the specific melting point temperatures (Primer Express, Applied BioSystems Software). To de-

termine absolute copy numbers of murine PECAM-1 and murine and human VEGF mRNA, individual cDNA templates were cloned and isolated and absolute mRNA copy numbers determined as described.[52] The SYBR Green 1 assay and the ABI Prism 7700 sequence detection system (Applied Biosystems) were used for detecting real-time quantitative PCR products from reverse-transcribed cDNA samples. Standard curves for each gene were plotted with quantified cDNA template and each target gene mRNA copy number normalized to 10^6 copies of cyclophilin control. The sequences of the PCR primer pairs (5′ to 3′) that were used for each gene are as follows: murine PECAM-1: forward, 5′-GAGCCCAATCACGTTTCAGTTT-3′ and reverse, 5′-TCCTTCCTGCTTCTTGCTAGCT-3′; murine VEGF: forward, 5′-GGAGATCCTCGAGGAGCACTT-3′ and reverse, 5′-GGCGATTTAGCAGCAGATATAAGAA-3′; murine cyclophilin: forward, 5′-CAGACGCCACTGTCGCTTT-3′ and reverse, 5′-TGTCTTTGGAACTTTGTCTGCAA-3′; human VEGF: forward, 5′-GCGGAGAAAGCATTTGTTTGT-3′ and reverse, 5′-CGGCTTGTCACATCTGCAA-3′; human cyclophilin: forward, 5′-CTGGACCCAACACAAATGGTT-3′ and reverse, 5′-CCACAATATTCATGCCTTCTTTCA-3′.

Ex Ova *Chicken Chorioallantoic Membrane (CAM) Assays for VEGF-Dependent Angiogenesis*

Chicken embryos were transferred from fertilized eggs to Petri dishes on gestation day 3, and maintained at 38°C with 90% humidity for the remainder of the study. On gestation day 7, ring-shaped nylon fabrics (3 nylons per CAM) were placed onto the CAMs and chicken DF-1 fibroblasts, either control or infected with RCAS virus vector[53] carrying the mVEGF cDNA[11] (25 μl of a cell concentration of 4×10^6 cells/ml), added to the nylon rings on each CAM. The RCAS vector derived from Rous sarcoma virus in which the *src* oncogene was deleted and replaced with a unique *Cla*I synthetic linker cloning site is a recombinant virus that can express foreign genes inserted into the *Cla*I site efficiently. On gestation day 10, and daily for the remainder of the study, 25 μl of control buffer (PBS) or test solution with indicated concentrations of NAC or angiostatin were added to the center of the nylon mesh rings. Five CAM's per test condition were studied. On day 16 of gestation, the resulting CAMs were evaluated for vessel morphology (eg, neovascularization) and harvested for histology (H&E). Additionally, nylon rings were excised, rinsed in saline, and frozen at −70°C for protein analysis. These frozen tissues were then processed for protein extract and analyzed for angiostatin levels using immunoblot as described above.

Statistical Analysis

Results from individual experiments are represented as mean ± SD unless otherwise stated. Statistical comparison of treatment groups was performed using two-tailed Student's *t*-test or Mann-Whitney test. Statistical significant was defined as $P < 0.05$.

Results

Systemic NAC Represses Primary Breast Cancer Tumor Growth and Viability

To determine the effect of NAC treatment on the growth of orthotopic breast cancer xenografts, MDA-MB-435 cells stably expressing GFP were injected subcutaneously into a single mammary fat pad of female athymic nude mice. When the tumors reached a palpable size of 3 to 4 mm in diameter, usually 10 days after implantation, the animals were randomized into treatment groups of 10 animals each; saline (vehicle control) and NAC (1 or 10 mg/kg/day) so that the mean tumor volume of each group was statistically equal. Tumor growth and animal weights were monitored throughout the 8-week treatment period. At the end of the treatment, tumors, axillary lymph nodes, and lung were harvested for histology, fluorescent microscopy, gene expression, and protein expression analyses.

Primary tumor growth was evaluated throughout time by measuring tumor dimensions externally through the skin with digital calipers through the course of the treatment and calculating volume based on ellipsoid ($\text{width}^2 \times \text{length} \times 0.52$). Interestingly, NAC (10 mg/kg/day)-treated animals displayed a repression of growth after tumors reached 125 mm^3 in size, and were statistically significant after 45 days of NAC treatment (Figure 1A). The final tumor volumes at 8 weeks averaged 225 ± 10 mm^3 for control and 150 ± 12 mm^3 for NAC treatment. No significant alterations in the body weight for all treatment groups were observed throughout the course of the experiment. Histochemical staining of the primary tumors showed a vast difference in the general architecture and significant central necrosis was apparent in the NAC-treated group compared to the control saline group (Figure 1C *versus* Figure 1B, respectively). The quantification of necrosis by histological grid analysis showed the NAC (10 mg/kg/day)-treated group was three times higher than the control group exceeding 50% of the total tumor area on average (Figure 1D). The progressive necrosis in the tumor center but not in the tumor edge of NAC-treated animals suggested selectivity for intratumor cell death, with little alteration in peripheral tumor viability. Animals treated with the low dose of NAC (1 mg/kg/day) showed intermediate values for tumor volumes and metastasis that were not statistically significant compared to the control group.

Systemic NAC Treatment Affects Tumor Metastasis to Lymph Nodes and Lung

Analysis of distal metastasis was facilitated by the use of a human metastatic breast cancer line, MDA-MB-435, that stably expresses GFP and can be detected at the single cell level. Axillary lymph node and lung tissues (whole mount gross and 5-μm sections) were analyzed by fluorescent microscopy to detect GFP-expressing tumor cells. Whole mount lymph nodes were analyzed directly after harvest for the presence of fluorescent foci

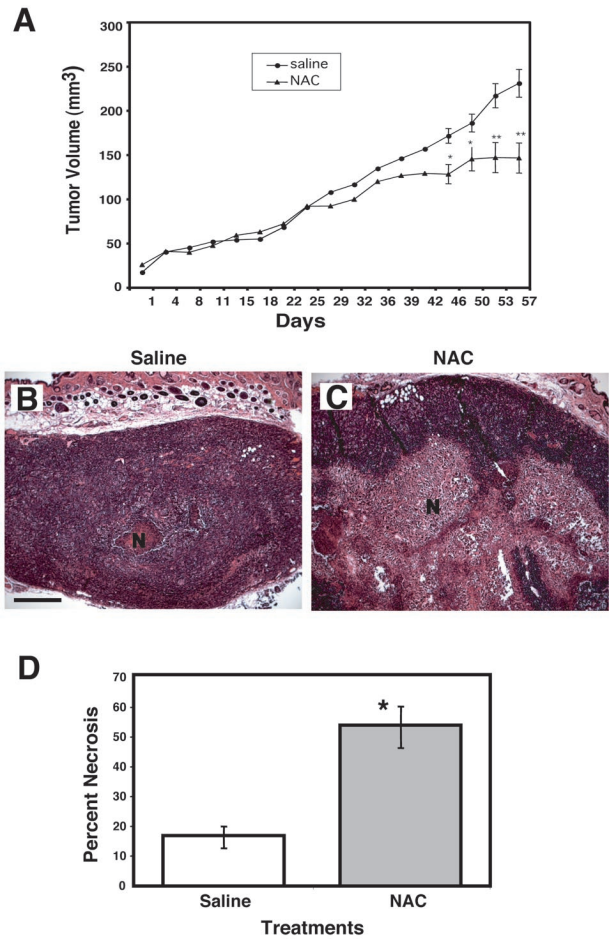

Figure 1. Primary orthotopic MDA-MB-435-GFP breast tumor growth and architecture with control and antioxidant treatment. **A:** Measurements of tumor growth for saline and NAC (10 mg/kg/day) for 8 weeks from start of treatment. Tumor volumes were calculated from external caliper measurements and $L \times W^2 \times 0.52$. Statistically significant differences between NAC and control saline indicated as $P < 0.05$ (*) and $P < 0.01$ (**). **B** and **C:** Representative tumor architecture for control saline (**B**) or NAC (10 mg/kg/day) (**C**). Internal tumor necrosis is indicated (N). **D:** Quantification of tumor necrotic area of saline vehicle and NAC-treated animals ($n = 10$); avg. ± SD. Statistical significance at $P < 0.01$ is indicated (*).

(Figure 2A, gross). Metastatic lesions in the lymph node were easily visualized in the saline groups whereas few or no cells were detected in the NAC-treated group. Histological sections were used to confirm individual GFP-expressing cells in the saline and NAC treatment groups (Figure 2A, section). Importantly, no metastatic GFP-expressing cells were detected in the contralateral axial lymph node away from the primary tumor, indicating a local lymphatic metastatic process similar to that observed in humans (data not shown). Quantification of the axillary lymph node metastasis was determined by fluorescent image analysis of histological sections of the nodes and showed that NAC repressed local metastasis by more than twofold (Figure 2C).

Distal metastasis to the lung indicated a similar profile of GFP-expressing breast cancer cells in which saline-treated animals revealed large foci of tumor inoculation and the NAC-treated group were significantly smaller and, if present, were mostly individual cells (Figure 2B, gross and section). Quantification of fluorescent foci in the lungs revealed a reduction in metastatic tumor foci despite the fact that no bias was given to individual foci size, identifying only total number of foci (Figure 2D). Thus, in addition to primary tumor viability, metastasis to lymph node and distal metastasis to lung were significantly inhibited by NAC treatment.

Systemic NAC Treatment Induces Tumor Cell Apoptosis and Loss of Intratumoral Microvascular Density

To evaluate whether the effect of NAC on tumor growth was operating through the induction of tumor cell apoptosis, we used histochemical staining of primary tumor sections by TUNEL assay (ApoTag). When compared to the saline group, NAC-treated tumors showed significant punctate dark brown stains as positive marker of cells undergoing DNA fragmentation and apoptosis (Figure 3A). The images were quantified by counting apoptotic cells and averaged for each treatment group ($n = 10$) (Figure 3B). The NAC-treated animals showed significantly increased cell apoptosis in the nonnecrotic areas (twofold increase), consistent with the associated loss in tumor viability. Interestingly, some of the apoptotic cells appeared to align with vascular capillary structures, indicating that the vasculature could be a target for NAC-induced apoptosis.

To address whether NAC treatment affects the vascular supply of experimental breast tumors, histological sections of the primary tumors were stained with a primarily endothelial-specific antibody against PECAM-1 (CD31). The CD31 staining showed that 4-week NAC-treated tumors, in the central viable areas, have a decreased vascular density by ~2.5-fold as compared to the saline control group (24.0 ± 1.23 *versus* 9.65 ± 1.93, respectively) (Figure 4A). Quantitative RT-PCR of tumors for the murine PECAM-1 marker showed a significant decrease in NAC-treated tumors as opposed to control (Figure 4B).

To examine whether endothelial cell-specific apoptosis was occurring in NAC-treated animals, sections were evaluated for endothelial cells undergoing apoptosis using CD31 immunostaining combined with TUNEL analysis. When compared with the control tumor sections (4.4 ± 0.5), NAC-treated tumors (7.4 ± 1.2) showed significant increases in endothelial cell apoptosis, even as early as 4 weeks, before the onset of necrosis (Figure 4C). These results suggest that NAC negatively affects the vascular compartment leading to tumor cell apoptosis.

Total VEGF mRNA and Protein Levels Were Moderately Repressed in the NAC-Treated Tumors

To assess whether NAC treatment affects the vascular compartment primarily through the repression of vascular maintenance factors such as VEGF, the levels of VEGF

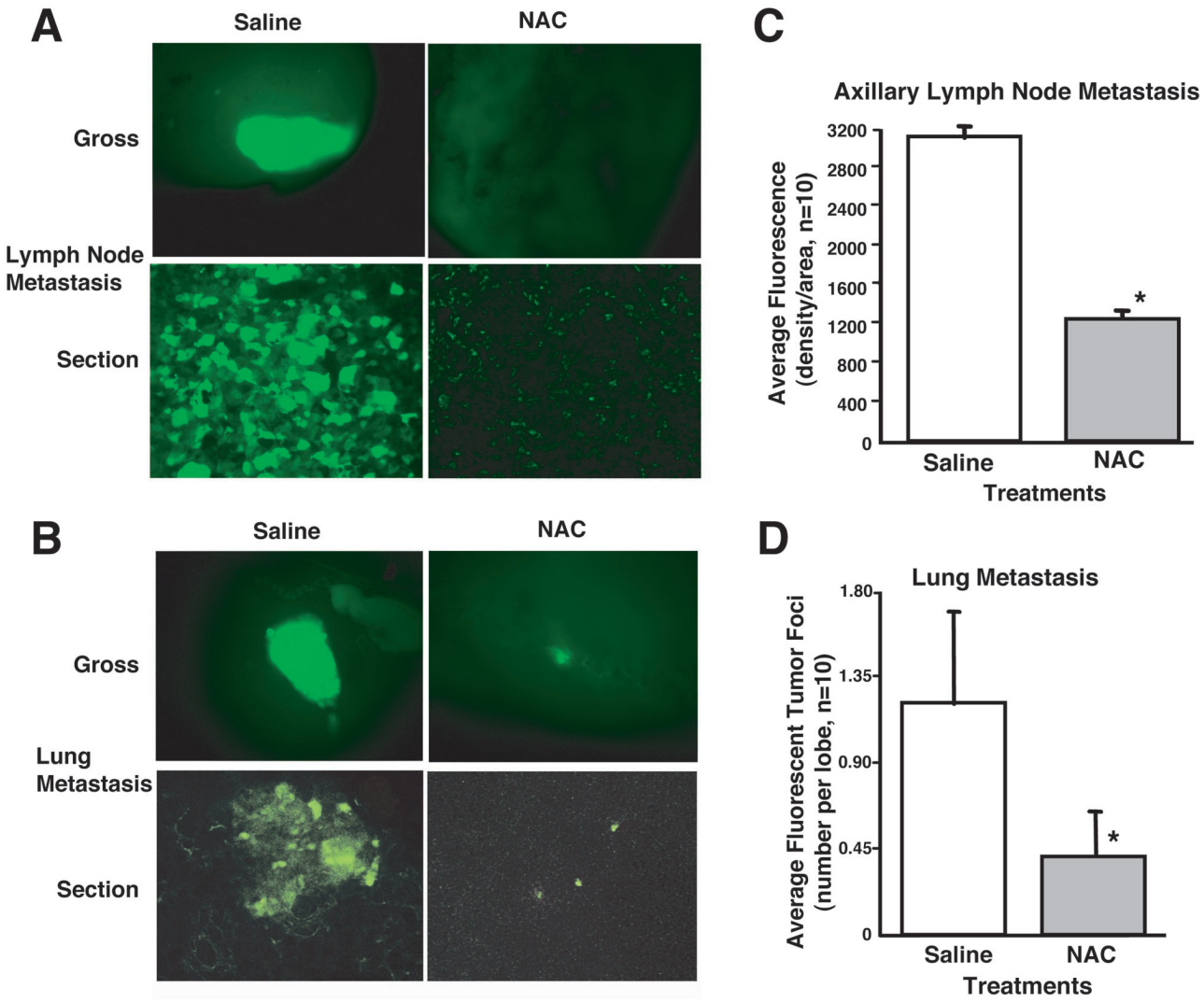

Figure 2. Secondary metastasis of fluorescent breast cancer cells to the lymph node and lung in tumor-bearing mice. **A:** Representative examples of axillary lymph node metastasis imaged with microscopic fluorescence in gross and cryosections (section) from saline and NAC-treated (10 mg/kg/day) mice. **B:** Lung metastatic foci of MDA-MB-435-GFP tumors with representative gross and microscopic fluorescent analysis of saline- and NAC-treated mice. Note: both the number and size of the fluorescent nodules/individual cells are dramatically reduced in the NAC-treated group. **C:** Quantification of fluorescent cellular area in histological cross-sections of axial lymph nodes from 10 tumor-bearing animals of each treatment group; saline, and NAC (10 mg/kg/day). Statistically significant difference from saline control indicated, $P < 0.01$ (*). **D:** Quantification of lung tumor foci metastasis with gross fluorescent microscopy. Comparison of saline and NAC matching the same group analyzed for lymph node metastasis above. Statistical significance from saline control as $P < 0.05$ is indicated (*); avg. ± SD.

mRNA and protein were evaluated in whole tumor extracts. Northern blot analysis of the 8-week MDA-MB-435 primary tumors for hVEGF-165, glucose transporter-1 (Glut-1), and ribosome-associated protein (36B4) are shown in Figure 5A for both saline- and NAC-treated animals. From densitometric analysis and normalization to 36B4, Glut-1 did not show any change in the steady state levels in either group but hVEGF showed a moderate 23% decrease in the NAC-treated tumors (0.115 ± 0.007) *versus* the saline-treated tumors (0.149 ± 0.004). Quantitative real-time RT-PCR was performed for human and murine VEGF to distinguish between tumor-derived VEGF and endogenous host-derived VEGF. The normalized values for human VEGF in saline- and NAC-treated tumors indicate that tumor-derived VEGF in the NAC group was repressed by 20% compared to saline control, similar to the reduction seen by Northern blot (Figure 5B). Contribution from host murine VEGF was nominal and did not seem to be dramatically regulated either way by NAC treatments, suggesting contribution by host-infiltrating cells are minimal. Total VEGF protein levels were assessed by a sensitive enzyme-linked immunosorbent assay and demonstrated a 10% reduction in NAC-treated tumors compared to saline controls (Figure 5C).

It is an important point to note, that these measurements were for total VEGF in the tumor. To examine focal and microenvironmental expression of VEGF, immunohistochemistry was performed on tumor sections (Figure 5D). The control saline tumors showed uniform VEGF expression whereas the NAC-treated group showed low VEGF in peripheral and high levels adjacent to the progressing necrosis. Thus, VEGF expression levels were counterbalanced to show a moderate overall decrease in the NAC-treated group.

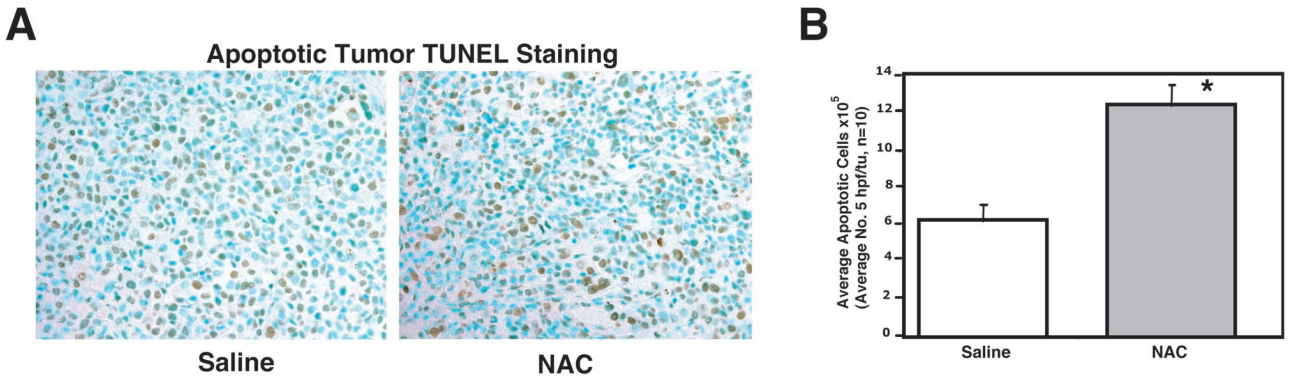

Figure 3. Quantitative analysis of total cellular apoptosis in control and NAC-treated tumors. **A:** Representative TUNEL staining of tumor histological sections obtained from viable areas of saline and NAC-treated tumors. **B:** Quantification of apoptotic cell count in tumor sections of saline and NAC-treated animals; avg. ± SD. Statistically significant difference of NAC *versus* saline control, $P < 0.01$ (*).

Systemic NAC Treatment Produces Increases in Endogenous Angiostatin in Primary Experimental Breast Tumors

NAC is a free sulfhydryl donor and has been shown to mediate proteolysis of human plasminogen to yield angiostatin ($K_{4.5}$; Mr 55,000 to 58,000) in the presence of plasminogen activator.[54] To test the hypothesis that NAC may reduce vascular maintenance via angiostatin-induced endothelial cell apoptosis in our animal model, immunohistochemical staining was performed for angiostatin in MDA-MB-435 experimental tumor sections (Figure 6A). Saline-treated tumors revealed focal positive staining selectively within tumor vessels that may be because of weak antibody cross-reactivity to plasminogen, as well as a low level of extravascular deposits. Systemic

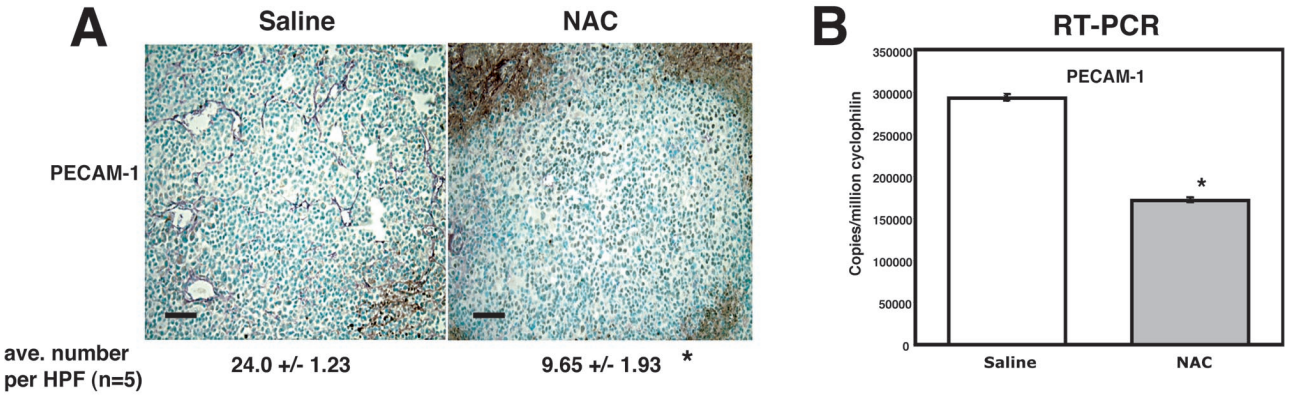

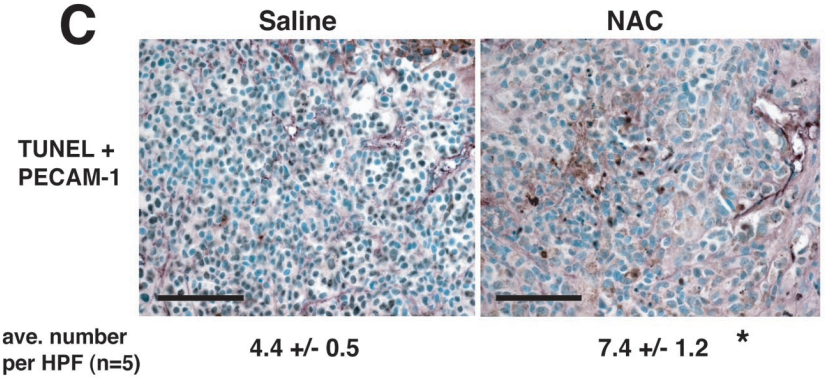

Figure 4. NAC treatment primarily results in vascular endothelial depletion and endothelial-specific apoptosis. **A:** Endothelial PECAM-1 staining and quantification in 8-week MDA-MB-435-GFP tumors in saline and NAC (10 mg/kg/day) treatment groups. Note the intratumoral necrosis surrounding PECAM-1-deficient but viable tumor areas. Histological quantification of PECAM-1-posititve staining in five tumors is shown below the representative images. **B:** Quantitative real-time RT-PCR analysis for murine PECAM-1 mRNA in three tumors per group shows significant repression with NAC treatments. Statistically significant difference from control saline indicated, $P < 0.01$(*). **C:** Representative staining and quantification of tumor histological slides co-stained for TUNEL (apoptosis) and PECAM-1 to quantify endothelial-specific apoptosis. Statistically significant difference from control, $P < 0.05$ (*). Scale bars, 100 μm.

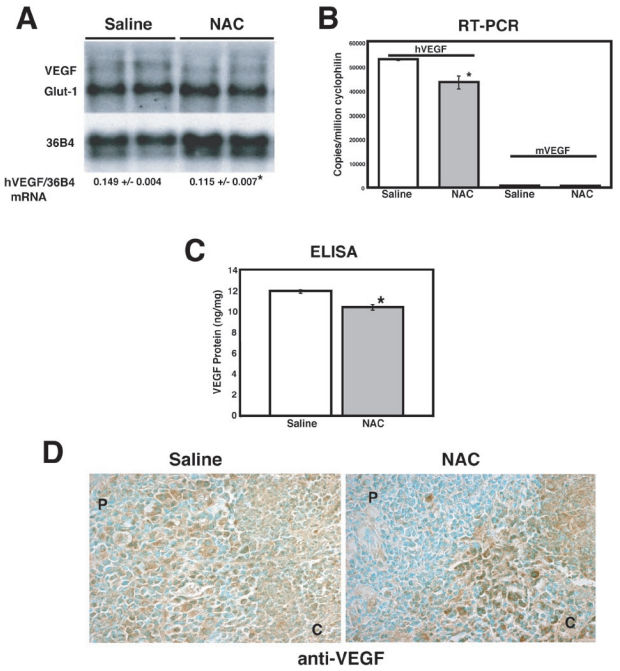

Figure 5. NAC moderately represses total VEGF expression. **A:** Evaluation and quantification of VEGF mRNA in saline and high-dose NAC-treated tumors. Representative Northern blot with hybridization signals for VEGF, Glut-1, and 36B4 control. Quantification of VEGF signal averaged and normalized with 36B4 for each lane for five tumors is shown below the blot. **B:** Quantitative RT-PCR using human VEGF primers and murine VEGF determined in triplicate tumor RNA samples. **C:** Quantification of VEGF protein levels using enzyme-linked immunosorbent assay analysis of total tumor protein extracts ($n = 5$ per group) indicates the level of VEGF reduced within the NAC group. Statistically significant from saline control is indicated, $P < 0.05$ (*); avg. ± SD. **D:** Representative immunohistochemical staining for human VEGF in central areas of tumors for saline or NAC. The saline-treated tumor section shows a uniform VEGF staining throughout the tumor whereas the NAC-treated tumor clearly shows a central hypoxic interface (C) where VEGF staining is focally increased and peripheral (P) areas where VEGF is absent.

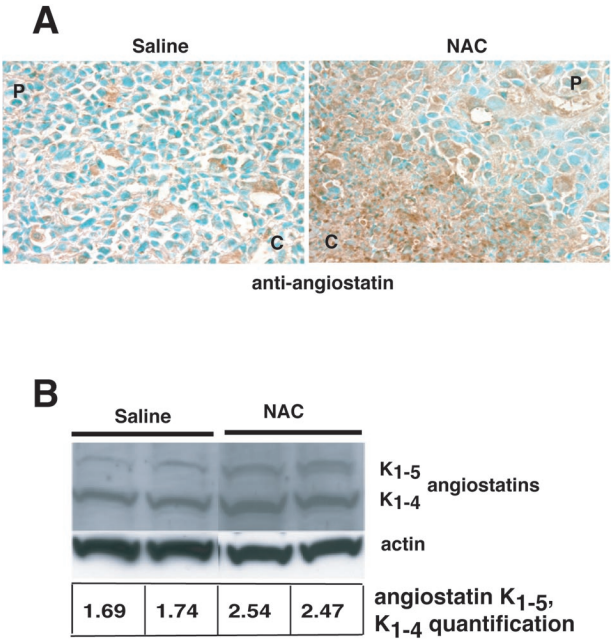

Figure 6. Orthotopic MDA-MB-435 breast tumors demonstrate increases in perivascular angiostatin with systemic NAC treatments. **A:** Immunohistochemistry for angiostatin in viable areas of tumors treated for 8 weeks with saline or NAC at 10 mg/kg/day. Central (C) and peripheral (P) areas are indicated. **B:** Western blot analysis of total tumor extracts for angiostatin fragments. Positive signal for angiostatin K_{1-5} and K_{1-4} are indicated, as well as signal for actin control. Quantification of angiostatin fragments compared to actin levels for each lane ($n = 5$) were determined.

NAC-treated tumors revealed a rather unique pattern of diffuse extravascular angiostatin deposition in the viable tumor, and intense and punctate angiostatin in the most central hypoxic regions. To confirm that this increase was in fact angiostatin in the NAC-treated tumors, immunoblot analysis of total protein extracts from saline- and NAC-treated animals was performed (Figure 6B). Both groups of MDA-MB-435 breast xenografts demonstrated the presence of angiostatin fragments, primarily the angiostatin kringle 1-4 and 1-5 isoforms. NAC-treated tumors showed a 37% increase in angiostatin compared to the saline controls when normalized to β-actin (2.34 ± 0.029 for NAC *versus* 1.71 ± 0.025 for saline). Hence, even though the immunoblot analysis necessarily includes whole tumor extracts, the NAC-dependent effect of increased angiostatin production suggests accumulation at focal locations within the core of tumors according to the immunohistochemical analysis.

Several reports have suggested that matrix metalloproteinases (MMPs) are important in facilitating the production of angiostatin in cells.[55,56] To examine potential involvement of MMP activation, total tumor extracts from saline- and NAC-treated tumors as well as conditioned medias from NAC-treated and control-untreated MDA-MB-435 cells showed no apparent changes in total or active MMP-2 or MMP-9 by zymographic analyses (data not shown). Thus, significant changes in MMP profiles could not be distinguished in these tumors or in cultured cells as indicated by other reports of Lewis lung carcinoma.[55]

VEGF and NAC Synergize to Promote Endothelial Cell Apoptosis through Angiostatin Production

The observation that, in the center of the tumor, VEGF expression in combination with NAC could induce endothelial cell apoptosis is consistent with the hypothesis that these effectors result in the focal accumulation of angiostatin, a potent apoptotic factor for endothelial cells. To elucidate whether NAC has the same effect *in vitro*, endothelial cell responses to VEGF in the absence or presence of NAC was evaluated. NAC, at levels relative to *in vivo* concentrations and in a dose-dependent manner, efficiently blocked VEGF-stimulated HUVEC viability, and at higher concentrations, induced cell apoptosis (Figure 7A). HUVEC apoptosis was confirmed by nuclear condensation observed in 4,6-diamidino-2-phenylindole-stained cells under the same treatments (data not shown). The addition of the proapoptotic factor, angiostatin alone, was able to induce a similar level of endothelial apoptosis, whereas NAC itself had no effect on HUVEC viability in the absence of VEGF. Hence, where VEGF typically promotes endothelial cell proliferation and sur-

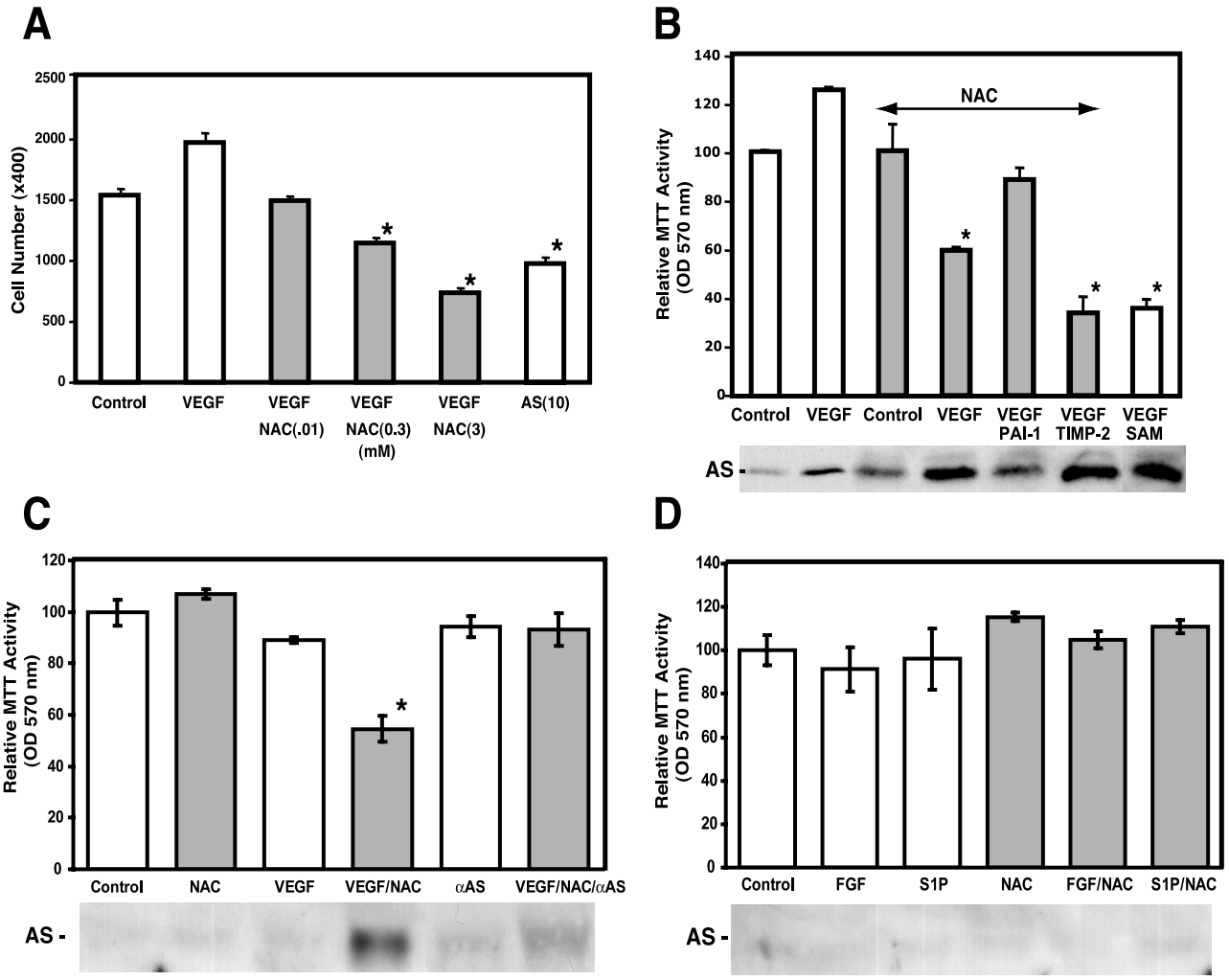

Figure 7. Endothelial cell apoptosis in response to combined VEGF and NAC treatment coincides with angiostatin production. **A:** HUVEC viability throughout 48 hours in low serum (3% FBS), in the presence of VEGF (10 ng/ml), and VEGF in combination with increasing concentrations of NAC (0.01, 0.3, and 3 mmol/L). Comparative reductions in HUVEC viability with the direct addition of angiostatin $K_{1\text{-}5}$ at 10 μg/ml [AS (10)]. Significantly different from VEGF alone, $P < 0.01$ (*). **B:** Cytokine- and NAC-induced endothelial apoptosis are VEGF-dependent and blocked by excess PAI-1, but not TIMP-2. HUVEC cell viability as measured by MTT assay, in the absence (**white bars**) and presence (**gray bars**) of NAC at 0.6 mmol/L, no treatment (control), or VEGF (10 ng/ml), PAI-1 (10 nmol/L), TIMP-2 (10 nmol/L), or VEGF (10 ng/ml) plus SAM alone (**white bar**) (SAM, 0.7 mmol/L). Statistically significant from control, $P < 0.01$ (*); avg. ± SD. **C:** HUVEC viability determined by MTT assay at 48 hours in 3% FBS no treatment (control), NAC at 0.6 mmol/L, VEGF (10 ng/ml), anti-angiostatin (1 μg/ml) (αAS), or combinations as indicated. Significantly different from VEGF alone, $P < 0.01$ (*). **D:** HUVEC viability determined by MTT assay at 48 hours in 3% FBS no treatment (control), FGF-2 (10 ng/ml), sphingosine-1-phosphate (S1P), and NAC at 0.6 mmol/L alone or in combination as indicated. Western blot analyses of nonreduced conditioned medias for total angiostatin production for each treatment condition (AS−) (**B–D**, bottom).

vival, VEGF in conjunction with NAC blocked endothelial cell viability at low doses and induced apoptosis with increasing NAC concentrations.

Because angiostatin was observed in the core of tumors treated with NAC, it was investigated whether angiostatin production could be responsible for the VEGF/NAC-induced endothelial cell apoptosis *in vitro*. HUVECs were treated with and without VEGF. As assessed by a parallel setup of MTT assay and immunoblot of cell culture-conditioned media, VEGF increased HUVEC viability and released a small amount of angiostatin into the media (Figure 7B). HUVECs treated with VEGF plus NAC showed a 48% loss in cell viability at 24 hours and resulted in a significant induction of angiostatin, primarily isoform $K_{1\text{-}5}$. However, when VEGF and NAC were combined with exogenous excess plasminogen activator inhibitor (PAI-1), the ability to induce endothelial cell apoptosis and increase angiostatin levels were inhibited, indicating that plasminogen activator activity is necessary for the accumulation of angiostatin. Alternatively, excess exogenous TIMP-2 added to the VEGF and NAC treatments promoted even more pronounced loss of cell viability and resulted in a higher level of angiostatin production. This serves to corroborate tumor cell and tumor extract zymographic results and indicates little MMP involvement in the production of angiostatin (data not shown). To test whether other thiol antioxidants could provide similar results as NAC, VEGF was combined with SAM, which also induced a significant loss of HUVEC viability concomitant with a coordinate increase in angiostatin release. Appropriate controls were performed in separate experiments to rule out effects of PAI-1, TIMP-2, and SAM alone on endothelial cells. Similar experiments combining VEGF with retinoic acid, selenium, or vitamin E

had little to no effect on endothelial cell viability (data not shown), indicating a specific requirement for thiol antioxidants.

In similar experiments, a polyclonal antibody raised against purified angiostatin was used to determine whether angiostatin was responsible for HUVEC apoptosis in the presence of VEGF and NAC. Confluent HUVEC cultures were treated with serum control, NAC, VEGF, and anti-angiostatin antibody alone and in combination as indicated in Figure 7C. As expected VEGF/NAC-treated HUVECs demonstrated appreciable loss of viability to 55% of the controls. However, VEGF/NAC and anti-angiostatin treatment did not result in endothelial apoptosis. Analysis of the conditioned medias from this experiment showed that as expected the accumulation of angiostatin was prominent in the VEGF/NAC treatment groups and very minimal in the controls.

Because VEGF is an effective mediator of cell survival, proliferation and gene expression in endothelial cells, it was unclear whether this activity was unique to VEGF or would occur with other endothelial growth factors or cell survival mediators. To test this possibility, FGF-2 and sphingosine-1-phosphate (S1P) were used in the viability assay with HUVECs with and without NAC treatment (Figure 7D). The activation of endothelial apoptosis in the presence of FGF-2 or S1P alone or in combination with NAC was not observed. Likewise, evaluation of conditioned medias from these experiments determined that little or no angiostatin was produced under these conditions in contrast to the observations with VEGF/NAC combinations. In additional control experiments, VEGF, FGF-2, and S1P all showed endothelial cell proliferative activity in subconfluent assays, demonstrating that they are functional HUVEC mediators at the concentration and batch used for these analyses (data not shown).

VEGF-Induced CAM Angiogenesis Is Blocked by NAC Co-Incident with Angiostatin Production

To model VEGF-dependent tumor angiogenesis *in vivo* and test the essential components of NAC-dependent anti-angiogenic activity, we used a VEGF-dependent angiogenesis assay in the differentiated chicken chorioallantoic membrane (CAM). Angiogenesis in this model is mediated by VEGF overexpression in chick fibroblasts implanted on the CAM, and is useful in evaluating anti-angiogenic activity of NAC or other compounds. In this modified CAM assay, 10-day fertilized chick eggs maintained in Petri dishes were used, to which were applied hole-punched nylon meshes containing chicken fibroblasts stably overexpressing VEGF. Saline, NAC, or angiostatin were then applied directly on the CAM within the confined circle of the mesh once a day for 7 days. *Trans*-illumination of the control VEGF CAM in the middle of the mesh showed a highly ordered neovasculature without significant vascular leakage or convoluted structures (VEGF) (Figure 8A). In contrast, when topical angiostatin (AS $_{K1-5}$) was added, the overall vascular order was disrupted and microvessels appeared to abruptly terminate as evident in the gross *trans*-illumination images (VEGF + AS $_{K1-5}$). A similar but more pronounced phenotype was observed with the addition of NAC (VEGF + NAC) (Figure 8A). Vascular perfusion studies with fluorescent high-molecular weight dextran tracer showed that topical angiostatin treatment induced abrupt small vessel blockage, whereas the NAC treatment induced both vessel termination and widespread vascular leakage and hemorrhaging (Figure 8A, FITC-dextran perfused). Hematoxylin and eosin (H&E) staining of paraffin-embedded CAMs revealed numerous dilated vessels in the control VEGF CAM. In contrast, smaller and constricted blood vessels with disparate leaking evident in the NAC-treated CAMs and a similar, effect with topical addition of angiostatin was observed (Figure 8A, H&E). Interestingly, the CAM sections showed a dramatic reduction in tissue thickness in NAC and angiostatin treatments, compared to control. Quantification of the angiogenic vascular counts alone, which do not account for defects in organization or function were evaluated independently (Figure 8B). VEGF-expressing CAMs had a high-vascular density as expected. Treatments with either NAC or angiostatin significantly reduced the total vessel number to nearly half the level of the VEGF controls.

To determine whether the CAM assay recapitulated the observations of angiostatin production by HUVEC cultures *in vitro*, we evaluated angiostatin levels in CAM protein extracts by immunoblot (Figure 8C). Control cell implants showed almost no plasmin or angiostatin fragments, whereas the VEGF-expressing cell implants have appreciable levels of both plasmin and angiostatin signals. When VEGF-expressing cells were topically treated with NAC, we observe a qualitative reduction in plasmin and concomitant increases in angiostatin fragments.

Thus, using this *in vivo* model, it was demonstrated that VEGF combined with NAC promotes vascular leakage and vessel termination. In addition, it is clear that the combination of VEGF and NAC promotes angiostatin production, leading to vascular depletion. Importantly, the use of other antioxidants such as selenium, vitamin C, and retinoic acid combined with VEGF did not alter the vascular phenotype in this model, indicating selectivity for thiol antioxidants (data not shown). This selectivity is consistent with the requirement for thiol antioxidants to promote the plasmin conversion to angiostatin.

Discussion

Antioxidants such as NAC have been known to be cytoprotective after exposure to cellular damaging agents such as reactive oxygen species.[36–38] NAC is a precursor to the cellular antioxidant glutathione (GSH), a scavenger for cell and DNA-damaging oxygen species such as hydrogen peroxide, superoxide, and lipid peroxides. In numerous studies, NAC and in particular GSH, have been shown to provide significant protection for stress-related cell and genomic damage. In addition, NAC has been found to be safe and efficacious in the clinic for treating acute respiratory distress and inflammation, as well as being a useful antidote for acute drug intoxica-

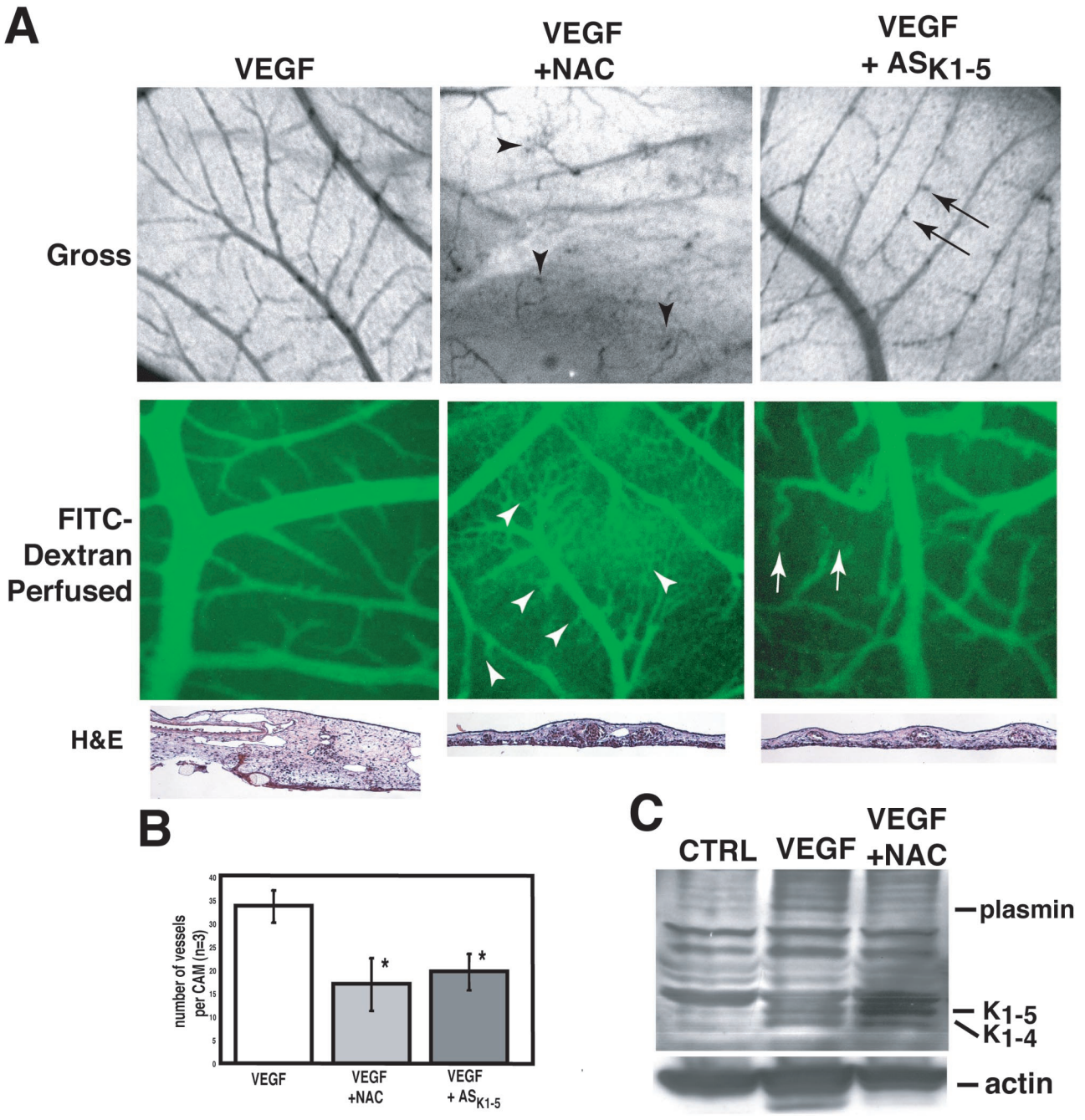

Figure 8. VEGF-driven angiogenesis in a CAM model is inhibited by NAC treatment coordinate with angiostatin production. **A:** Image analysis of CAM vasculature that is activated by VEGF-expressing chicken fibroblasts implanted in a mesh ring. Photographs (gross) of the center area of the implant are shown for VEGF-cells alone or with topical addition of NAC (10 μg/implant/day) (VEGF + NAC) or angiostatin $K_{1\text{-}5}$ (AS $K_{1\text{-}5}$, 1 μg/implant/day) (VEGF + $AS_{K1\text{-}5}$) for 5 days. Note the acute branching/termination in the NAC-treated groups (**arrowheads**) and abrupt termination in the angiostatin-treated CAM (**arrows**). Fluorescent perfusion and vascular imaging with intravenous FITC-dextran at 5 days of treatment. VEGF + NAC show both vascular branching, leakage, and terminating vessels (**arrowheads**). Topical addition of angiostatin revealed predominantly abrupt terminating vessels with minor leakage (**arrows**). Histological profile of CAMs from the various treatments are shown below the vessel network images (H&E); VEGF demonstrated an expanded CAM with a multitude of dilated vessels, VEGF plus NAC shows a condensed CAM and few dilated vessels, and VEGF plus angiostatin shows a similar pattern with dramatic loss of cell density. **B:** Quantification of microvascular density throughout the entire CAM within the circle implant with VEGF-expressing cells alone or VEGF cells plus topical NAC or angiostatin (VEGF + $AS_{K1\text{-}5}$). Statistically significant difference from VEGF alone, $P < 0.05$ (*). **C:** Analysis of CAM total protein extracts show increases in angiostatin production with NAC treatments. Nonreducing Western blot of total extracts shows angiostatin fragments ($K_{1\text{-}5}$ and $K_{1\text{-}4}$) in VEGF lanes and increases in $K_{1\text{-}5}$ in VEGF combined with NAC. Actin is included as a loading control. Original magnification, ×2.0 (**A**).

tion.[43,57,58] The potential for antioxidants to be effective adjuvant therapies for the treatment of solid tumors and possible mechanisms of action in experimental tumorigenic models have yet to be determined.

Recent studies have suggested that NAC may have potential as an anti-tumorigenic agent with efficacy in preventing initial tumor take and metastasis along with a repression of VEGF expression in an experimental Kar-

posi sarcoma model.[44,60] The data presented here indicated that NAC treatment does repress the level of VEGF expression in experimental breast tumors. However, the moderate level of repression did not necessarily explain the significant loss in tumor viability. In addition, it was apparent that VEGF expression was still significant in hypoxic tumor microenvironments, thus defining focal areas of high VEGF expression. The efficacy of NAC on the growth and viability of human breast carcinoma xenografts indicated that it is the tumor center that was predominantly affected by systemic NAC treatment, particularly with a dramatic loss of intratumoral vascular maintenance. Our observations suggest that NAC does not primarily affect the initial formation of neovessels because the vascularity in the periphery of the tumors was unaffected by NAC, indicating selective NAC efficacy in established tumors.

An interesting result of the vascular depletion in the center of the tumor was that metastasis to draining lymph nodes was also affected. Tumor cell metastasis in this model seems to have a significant component that relies on the intratumoral vasculature and/or tumor cell viability. In addition it has been shown that NAC has direct effects on tumor cell metastasis, which has been described by others.[39] Despite these observations, the moderate repression of VEGF by NAC might only partially explain the extent of intratumoral necrosis observed.

The discovery of endogenous angiogenic inhibitors selective for endothelial cells has been pioneered by the discovery of the plasminogen fragment, angiostatin,[28,29,54] and subsequently expanded to numerous factors including endostatin, tumstatin, and thrombospondin peptides.[27,30,31] The focus of interest in the field of therapeutic tumor anti-angiogenesis is the potential to modulate the balance between endogenous angiogenic inhibitors and positive angiogenic factors. Here, a novel mechanism is described whereby the potent angiogenic activator VEGF is repressed with NAC treatment in peripheral areas, and expression of VEGF along with NAC in hypoxic areas in the core of established tumors promotes the production of the endothelial apoptotic factor, angiostatin. Consequently angiostatin acts *in situ* to block blood vessel formation and maintenance by selectively inducing vascular endothelial cells to apoptose (Figure 9).

Determination of mechanisms that may be operating in a temporal manner and/or within local tumor microenvironments during tumor expansion and metastasis is a difficult endeavor. Clearly, NAC has cytoprotective activities in numerous cell types as defined by *in vitro* stress models.[43] In these studies, a direct repression of endothelial cell viability was observed with the combined therapy of VEGF and NAC. Activation of endothelial cells by VEGF has been shown to result in the induction of active urokinase plasminogen activator[20,21,59] and defines the connection between VEGF action and NAC-promoting angiostatin production. *In vitro* experiments have demonstrated the efficacy of thiol antioxidants in promoting the conversion of plasminogen into angiostatin in the presence of plasminogen activator, a key component of this conversion cascade.[45]

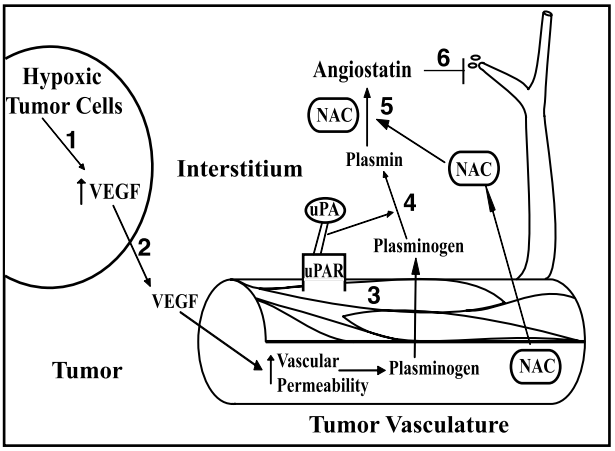

Figure 9. Model for the tumor microenvironment and NAC activation of endothelial apoptosis through VEGF-dependent angiostatin production. Stepwise events contributing to intratumoral angiostatin production by NAC treatment: **1:** Central tumor vascular supply cannot support tumor cell metabolic demand resulting in focal hypoxia and VEGF production. **2:** Secreted VEGF diffuses within the local interstitium to activate local tumor capillaries. **3:** Endothelial cells respond to VEGF with greatly increased permeability (ie, extravasation of plasminogen, NAC) and up-regulation of uPAR-uPA on the endothelial cell membrane. **4:** Active uPA converts plasminogen substrate into active plasmin. **5:** Excess NAC promotes degradation of plasmin into angiostatin. **6:** Angiostatin induces endothelial cell apoptosis, loss of new capillary extension, and maintenance.

Angiostatin accumulates in certain tumor cell types and has been correlated with MMP activity in a model of concomitant resistance, such as Lewis lung carcinoma.[55] Interestingly, NAC was found to be ineffective in preventing Lewis lung carcinoma tumor inoculation and metastasis.[39] The *in vitro* studies indicate that, the local production of angiostatin that is promoted by VEGF activation of endothelial cells in the presence of NAC, does not require MMP activity, because excess TIMP-2 did not affect the VEGF/NAC-induced apoptosis. It is likely that plasminogen activation in the presence of NAC and degradation of plasmin through MMP activity are both potential pathways of angiostatin accumulation. Thus, MMP expression and activation profiles, hypoxia-induced VEGF expression, and endothelial/tumor cell expression of plasminogen activators are all factors that might contribute to angiostatin production and/or tumor sensitivity to NAC treatment.

VEGF is a potent permeability factor induced by hypoxia and may have a crucial function in promoting angiostatin accumulation in the presence of NAC. Vascular permeability at the local tumor microenvironment where high levels of VEGF are secreted results in the extravasation of circulating factors, one of which would be plasminogen, the substrate for plasminogen activator. Coordinately, VEGF is known to activate cell surface plasminogen activator activity through the induction of urokinase plasminogen activator receptor and urokinase plasminogen activator in endothelial cells. Thus, the extravasated plasminogen and VEGF-induced endothelial uPA activity promotes the production of plasmin, and in the presence of NAC, conversion to angiostatin. In summary, the unique combination of these events coalesce to provide an intratumoral microenvironment responsible for the induction of VEGF expression, endothelial activation,

vascular permeability, plasminogen extravasation, endothelial plasminogen activator activity, plasmin production, and in the presence of NAC or other thiol antioxidants, the promotion of the endothelial apoptotic factor, angiostatin, and vascular depletion (Figure 9). It is these events and unique requirements that might be proposed to predict the efficacy of NAC on the angiogenic processes. NAC efficacy will likely have constraints on tumor growth parameters, tumor size, and dependence on intratumoral vascular networks. The interesting observation that VEGF was highly effective in promoting angiostatin production and HUVEC apoptosis when compared to either FGF-2 or S1P may be related to the level of endothelial cell uPA/uPAR production promoted by VEGF as opposed to FGF-2 and other cytokines, a possibility currently being tested.[59]

One interesting prospect derived from these observations is the potential for treating tumor-bearing patients with high-dose adjuvant thiol antioxidants to facilitate intratumoral vascular depletion and necrosis. In conjunction, the standard chemotherapeutic modalities could be used to target the highly vascularized and oxygenated tumor peripheral sites that are likely to be resistant to antioxidant therapy.

Acknowledgments

We thank Timothy Hla, Donald Kreutzer, and Gerald Soff for helpful scientific discussions and advice; and Tatiana Estrada-Hernandez, Nancy Ryan, and Susan Kavel for technical support.

References

1. Folkman J: Tumor angiogenesis: therapeutic implications. N Engl J Med 1971, 285:1182–1186
2. Folkman J: Anti-angiogenesis: new concept for therapy of solid tumors. Ann Surg 1972, 175:409–416
3. Kim KJ, Li B, Winer J, Armanini M, Gillett N, Phillips HS, Ferrara N: Inhibition of vascular endothelial growth factor-induced angiogenesis suppresses tumor growth in vivo. Nature 1993, 362:841–844
4. Jain RK: Tumor angiogenesis and accessibility: role of vascular endothelial growth factor. Semin Oncol 2002, 29 (6 Suppl 16):3–9
5. Dvorak HF, Nagy JA, Feng D, Brown LF, Dvorak AM: Vascular permeability factor/vascular endothelial growth factor and the significance of microvascular hyperpermeability in angiogenesis. Curr Top Microbiol Immunol 1999, 237:97–132
6. Gasparini G: Prognostic value of vascular endothelial growth factor in breast cancer. Oncologist 2000, 5(Suppl 1):37–44
7. Toi M, Inada K, Suzuki H, Tominaga T: Tumor angiogenesis in breast cancer: its importance as a prognostic indicator and the association with vascular endothelial growth factor expression. Breast Cancer Res Treat 1995, 36:193–204
8. Fujimoto J, Sakaguchi H, Aoki I, Khatun S, Tamaya T: Clinical implications of expression of vascular endothelial growth factor in metastatic lesions of ovarian cancers. Br J Cancer 2001, 85:313–316
9. Karayiannakis AJ, Bolanaki H, Syrigos KN, Asimakopoulos B, Polychronidis A, Anagnostoulis S, Simopoulos C: Serum vascular endothelial growth factor levels in pancreatic cancer patients correlate with advanced and metastatic disease and poor prognosis. Cancer Lett 2003, 194:119–124
10. Claffey KP, Wilkison WO, Spiegelman BM: Vascular endothelial growth factor. Regulation by cell differentiation and activated second messenger pathways. J Biol Chem 1992, 267:16317–16322
11. Claffey KP, Robinson GS: Regulation of VEGF/VPF expression in tumor cells: consequences for tumor growth and metastasis. Cancer Metastasis Rev 1996, 15:165–176
12. Graham CH, Fitzpatrick TE, McCrae KR: Hypoxia stimulates urokinase receptor expression through a heme protein-dependent pathway. Blood 1998, 91:3300–3307
13. Shih SC, Mullen A, Abrams K, Mukhopadhyay D, Claffey KP: Role of protein kinase C isoforms in phorbol ester-induced vascular endothelial growth factor expression in human glioblastoma cells. J Biol Chem 1999, 274:15407–15414
14. Berra E, Pages G, Pouyssegur J: MAP kinases and hypoxia in the control of VEGF expression. Cancer Metastasis Rev 2000, 19:139–145
15. Semenza GL: HIF-1: using two hands to flip the angiogenic switch. Cancer Metastasis Rev 2000, 19:59–65
16. Kim I, Moon SO, Kim SH, Kim HJ, Koh YS, Koh GY: Vascular endothelial growth factor expression of intercellular adhesion molecule 1 (ICAM-1), vascular cell adhesion molecule 1 (VCAM-1), and E-selectin through nuclear factor-kappa B activation in endothelial cells. J Biol Chem 2001, 276:7614–7620
17. Lu M, Perez VL, Ma N, Miyamoto K, Peng HB, Liao JK, Adamis AP: VEGF increases retinal vascular ICAM-1 expression in vivo. Invest Ophthalmol Vis Sci 1999, 40:1808–1812
18. Bernatchez PN, Soker S, Sirois MG: Vascular endothelial growth factor effect on endothelial cell proliferation, migration, and platelet-activating factor synthesis is Flk-1-dependent. J Biol Chem 1999, 274:31047–31054
19. Ferrara N: Role of vascular endothelial growth factor in physiologic and pathologic angiogenesis: therapeutic implications. Semin Oncol 2002, 29:10–14
20. Pepper MS, Ferrara N, Orci L, Montesano R: Vascular endothelial growth factor (VEGF) induces plasminogen activators and plasminogen activator inhibitor-1 in microvascular endothelial cells. Biochem Biophys Res Commun 1991, 181:902–906
21. Mandriota SJ, Seghezzi G, Vassalli JD, Ferrara N, Wasi S, Mazzieri R, Mignatti P, Pepper MS: Vascular endothelial growth factor increases urokinase receptor expression in vascular endothelial cells. J Biol Chem 1995, 270:9709–9716
22. Pepper MS: Role of the matrix metalloproteinase and plasminogen activator-plasmin systems in angiogenesis. Arterioscler Thromb Vasc Biol 2001, 21:1104–1117
23. Behzadian MA, Windsor LJ, Ghaly N, Liou G, Tsai NT, Caldwell RB: VEGF-induced paracellular permeability in cultured endothelial cells involves urokinase and its receptor. EMBO J 2003, 17:752–754
24. Rakic JM, Maillard C, Jost M, Bajou K, Masson V, Devy L, Lambert V, Foidart JM, Noel A: Role of plasminogen activator-plasmin system in tumor angiogenesis. Cell Mol Life Sci 2003, 60:463–473
25. Kaneko T, Konno H, Baba M, Tanaka T, Nakamura S: Urokinase-type plasminogen activator expression correlates with tumor angiogenesis and poor outcome in gastric cancer. Cancer Sci 2003, 94:43–49
26. Hattenbach LO, Allers A, Gumbel HO, Scharrer I, Koch FH: Vitreous concentrations of TPA and plasminogen activator inhibitor are associated with VEGF in proliferative diabetic vitreoretinopathy. Retina 1999, 19:383–389
27. Jimenez B, Volpert OV, Crawford SE, Febbraio M, Silverstein RL, Bouck N: Signals leading to apoptosis-dependent inhibition of neovascularization by thrombospondin-1. Nat Med 2000, 6:41–48
28. O'Reilly MS, Holmgren L, Shing Y, Chen C, Rosenthal RA, Cao Y, Moses M, Lane WS, Sage EH, Folkman J: Angiostatin: a circulating endothelial cell inhibitor that suppresses angiogenesis and tumor growth. Cold Spring Harb Symp Quant Biol 1994, 59:471–482
29. O'Reilly MS, Holmgren L, Shing Y, Chen C, Rosenthal RA, Moses M, Lane WS, Cao Y, Sage EH, Folkman J: Angiostatin: a novel angiogenesis inhibitor that mediates the suppression of metastases by a Lewis lung carcinoma. Cell 1994, 79:315–328
30. O'Reilly MS, Boehm T, Shing Y, Fukai N, Vasios G, Lane WS, Flynn E, Birkhead JR, Olsen BR, Folkman J: Endostatin: an endogenous inhibitor of angiogenesis and tumor growth. Cell 1997, 88:277–285
31. Maeshima Y, Sudhakar A, Lively JC, Ueki K, Kharbanda S, Kahn CR, Sonenberg N, Hynes RO, Kalluri R: Tumstatin, an endothelial cell-specific inhibitor of protein synthesis. Science 2002, 295:140–143
32. Moser TL, Stack MS, Asplin I, Enghild JJ, Hojrup P, Everitt L, Hubchak S, Schnaper HW, Pizzo SV: Angiostatin binds ATP synthase on the surface of human endothelial cells. Proc Natl Acad Sci USA 1999, 96:2811–2816

33. Moser TL, Kenan DJ, Ashley TA, Roy JA, Goodman MD, Misra UK, Cheek DJ, Pizzo SV: Endothelial cell surface F1–F0 ATP synthase is active in ATP synthesis and is inhibited by angiostatin. Proc Natl Acad Sci USA 2001, 98:6656–6661
34. Redlitz A, Daum G, Sage EH: Angiostatin diminishes activation of the mitogen-activated protein kinases ERK-1 and ERK-2 in human dermal microvascular endothelial cells. J Vasc Res 1999, 36:28–34
35. Wahl ML, Owen CS, Grant DS: Angiostatin induces intracellular acidosis and anoikis in endothelial cells at a tumor-like low pH. Endothelium 2002, 9:205–216
36. Baas P, Oppelaar H, van der Valk MA, van Zandwijk N, Stewart FA: Partial protection of photodynamic-induced skin reactions in mice by N-acetylcysteine: a preclinical study. Photochem Photobiol 1994, 59:448–454
37. Emonet-Piccardi N, Richard MJ, Ravanat JL, Signorini N, Cadet J, Beani JC: Protective effects of antioxidants against UVA-induced DNA damage in human skin fibroblasts in culture. Free Radic Res 1998, 29:307–313
38. De Flora S, Izzotti A, D'Agostini F, Balansky RM: Mechanisms of N-acetylcysteine in the prevention of DNA damage and cancer, with special reference to smoking-related end-points. Carcinogenesis 2001, 22:999–1013
39. Albini A, D'Agostini F, Giunciuglio D, Paglieri I, Balansky R, De Flora S: Inhibition of invasion, gelatinase activity, tumor take and metastasis of malignant cells by N-acetylcysteine. Int J Cancer 1995, 61:121–129
40. Aluigi MG, De Flora S, D'Agostini F, Albini A, Fassina G: Antiapoptotic and antigenotoxic effects of N-acetylcysteine in human cells of endothelial origin. Anticancer Res 2000, 20:3183–3187
41. De Flora S, D'Agostini F, Masiello L, Giunciuglio D, Albini A: Synergism between N-acetylcysteine and doxorubicin in the prevention of tumorigenicity and metastasis in murine models. Int J Cancer 1996, 67:842–848
42. D'Agostini F, Bagnasco M, Giunciuglio D, Albini A, De Flora S: Inhibition by oral N-acetylcysteine of doxorubicin-induced clastogenicity and alopecia, and prevention of primary tumors and lung micrometastases in mice. Int J Oncol 1998, 13:217–224
43. Zafarullah M, Li WQ, Sylvester J, Ahmad M: Molecular mechanisms of N-acetylcysteine actions. Cell Mol Life Sci 2003, 60:6–20
44. Albini A, Morini M, D'Agostini F, Ferrari N, Campelli F, Arena G, Noonan DM, Pesce C, De Flora S: Inhibition of angiogenesis-driven Kaposi's sarcoma tumor growth in nude mice by oral N-acetylcysteine. Cancer Res 2001, 61:8171–8178
45. Gately S, Twardowski P, Stack MS, Cundiff DL, Grella D, Castellino FJ, Enghild J, Kwaan HC, Lee F, Kramer RA, Volpert O, Bouck N, Soff GA: The mechanism of cancer-mediated conversion of plasminogen to the angiogenesis inhibitor angiostatin. Proc Natl Acad Sci USA 1997, 94:10868–10872
46. Price JE, Polyzos A, Zhang RD, Daniels LM: Tumorigenicity and metastasis of human breast carcinoma cell lines in nude mice. Cancer Res 1990, 50:717–721
47. Skobe M, Hawighorst T, Jackson DG, Prevo R, Janes L, Velasco P, Riccardi L, Alitalo K, Claffey K, Detmar M: Induction of tumor lymphangiogenesis by VEGF-C promotes breast cancer metastasis. Nat Med 2001, 7:192–198
48. Hendrix MJ, Seftor EA, Seftor RE, Fidler IJ: A simple quantitative assay for studying the invasive potential of high and low human metastatic variants. Cancer Lett 1987, 38:137–147
49. Maciag T, Hoover GA, Stemerman MB, Weinstein R: Serial propagation of human endothelial cells in vitro. J Cell Biol 1981, 91:420–426
50. Maciag T, Kadish J, Wilkins L, Stemerman MB, Weinstein R: Organizational behavior of human umbilical vein endothelial cells. J Cell Biol 1982, 94:511–520
51. Shih SC, Claffey KP: Role of AP-1 and HIF-1 transcription factors in TGF-beta activation of VEGF expression. Growth Factors 2001, 19: 19–34
52. Shih SC, Robinson GS, Perruzzi CA, Calvo A, Desai K, Green JE, Ali IU, Smith LE, Senger DR: Molecular profiling of angiogenesis markers. Am J Pathol 2002, 161:35–41
53. Hughes SH, Greenhouse JJ, Petropoulos CJ, Sutrave P: Adapter plasmids simply the insertion of foreign DNA into helper-independent retroviral vectors. J Virology 1987, 61:3004–3012
54. Soff GA: Angiostatin and angiostatin-related proteins. Cancer Metastasis Rev 2000, 19:97–107
55. O'Reilly MS, Wiederschain D, Stetler-Stevenson WG, Folkman J, Moses MA: Regulation of angiostatin production by matrix metalloproteinase-2 in a model of concomitant resistance. J Biol Chem 1999 274:29568–29571
56. Pozzi A, Moberg PE, Miles LA, Wagner S, Soloway P, Gardner HA: Elevated matrix metalloprotease and angiostatin levels in integrin alpha 1 knockout mice cause reduced tumor vascularization. Proc Natl Acad Sci USA 2000, 97:2202–2207
57. Woo OF, Mueller PD, Olson KR, Anderson IB, Kim SY: Shorter duration of oral N-acetylcysteine therapy for acute acetaminophen overdose. Ann Emerg Med 2000, 35:363–368
58. Bird SB, Mazzola JL, Brush DE, Boyer EW, Aaron CK: A prospective evaluation of abbreviated oral N-acetylcysteine (NAC) therapy for acetaminophen poisoning. Acad Emerg Med 2003, 10:521
59. Mandriota SJ, Pepper MS: Vascular endothelial growth factor-induced in vitro angiogenesis and plasminogen activator expression are dependent on endogenous basic fibroblast growth factor. J Cell Sci 1997, 110:2293–2302
60. Cai T, Fassina G, Morini M, Aluigi MG, Masiello L, Fontanini G, D'Agostini F, De Flora S, Noonan DM, Albini A: N-acetylcysteine inhibits endothelial cell invasion and angiogenesis. Lab Invest 1999, 79:1151–1159